A threshold stress for pressure solution creep in rock salt: Model predictions vs. observations

B.G.A. van Oosterhout[1]*, S.J.T. Hangx[1], C.J. Spiers[1]

[1]HPT-laboratory, Department of Earth Sciences, Faculty of Geosciences, Utrecht University, The Netherlands

* b.g.a.vanoosterhout@uu.nl

ABSTRACT: At low deviatoric stress, flow of rock salt is expected to be controlled by pressure solution creep. This requires a fluid phase to be present in grain boundaries in the form of adsorbed grain boundary films or a dynamically wetting island-channel structure. However, whether such structures can persist at low stress or will be eliminated by healing phenomena is open to question. In this study, a model is derived describing a threshold stress for pressure solution, below which healing occurs, and creep is stopped. The results predict that pressure solution creep in rock salt, at depths up to 3 km, is inhibited below a deviatoric stress of 0.07 to 0.7 or at most 0.90 MPa. When deviatoric stresses in rock salt drop below this threshold stress, a decrease in strain rate from $\sim 10^{-13}$ to 10^{-18} s^{-1} is expected, due to a switch to dislocation creep. The model needs to be tested against CT experiments or optical observations on grain boundary behavior under stress, and against confined creep tests at very low deviatoric stress, as far as technically feasible. If confirmed, the effect of this threshold stress needs to be considered in future numerical studies of flow in rock salt.

1   Introduction

Creep laws for rock salt provide essential input for modelling salt tectonic flow, the long-term evolution of salt-based radioactive waste repositories (Tsang et al. 2005), solution-mined cavern behavior and associated subsidence (Breunese et al. 2003), and closure of uncased (abandoned) wellbores in rock salt (Orlic & Buijze 2014). At laboratory strain rates, temperatures of 20-200°C and differential (deviatoric) stresses in the range 5-25 MPa, deformation of natural rock salt is characterized by power-law dislocation creep with a stress sensitivity (n-value) of typically ~5 (Carter & Hansen 1983; Hunsche & Hampel 1999). However, strain rates inferred from field studies are several orders of magnitude higher than expected from extrapolating laboratory dislocation creep laws to natural, low-stress conditions (Urai et al. 1986; Bérest et al. 2019). This suggests that another mechanism, with a lower stress exponent (n), controls creep in rock salt at deviatoric stresses below 4-5 MPa.

A likely candidate, based on theory and on experiments on synthetic fine-grained (50-200 µm) salt is fluid-assisted grain boundary diffusion creep, or "pressure solution (Spiers et al. 1990). The rate of creep by this linear viscous mechanism (n=1) is inversely proportional to grain size cubed. For this reason, it is extremely slow and difficult to detect in experiments on natural salt (grain size 3-10 mm). Nonetheless, strong evidence for this type of behavior has recently been reported in ultra-long term (years), mostly unconfined creep tests, performed on natural salts at differential stresses down to ~1 or even 0.1 MPa under stable environmental conditions (Bérest et al. 2019; Herchen et al 2018). On the other hand, microstructural observations (Urai et al. 1986; 1987; Peach et al. 2001; Schleder & Urai 2007), thermodynamic arguments (Desbois et al. 2012) and observations on sinking rates of anhydrite rafts or "stringers" in salt formations (Raith et al. 2016) have been taken to imply that a threshold stress of 1-10 MPa exists below which pressure solution does not operate in salt under (confined) subsurface conditions - due to healing of the grain boundary fluid films that make pressure solution possible.

If linear (pressure solution) creep indeed occurs at low deviatoric stresses in the far field around salt caverns, storage facilities and boreholes, then the long-term evolution of these systems

and associated surface and/or environmental effects, will be impacted and need to be evaluated. Both microphysically (Spiers et al. 1990) and experimentally based (Bérest et al. 2019, Herchen et al. 2018) linear creep laws that account for pressure solution already exist and have been applied and tuned in numerical simulations of cavern convergence and subsidence (e.g. Breunese et al 2003). In contrast, no experimental evidence has been found for the existence of a threshold stress below which pressure solution is prevented by grain boundary healing, at least down to a few MPa in confined creep tests at in-situ conditions (Herchen et al. 2018) and to 0.2 MPa in unconfined tests (Berest et al. 2019). Moreover, previous thermodynamic estimates (1-10 MPa - Desbois et al. 2012) are based on a model that is appropriate for quartz but less so for salt. The aim of the present paper is to derive a theoretical criterion for the threshold stress for pressure solution that accounts for the specific properties of rock salt and that can be tested in future via targeted experiments.

2   Previous work

Creep of a dense polycrystalline material by pressure solution requires a fluid phase to be #present in grain boundaries in the form of adsorbed grain boundary films (Rutter 1976) or else a dynamically wetting (non-equilibrium) island-channel network (Lehner 1990) as inferred for wet salt by Spiers et al. (1990) and De Meer et al. (2002) (Figure 1a-c). Pressure solution in such a system is driven by chemical potential gradients around individual grains, set up by gradients in normal stress. It involves three serial processes: (1) dissolution of the solid at grain boundaries under high normal stress, (2) diffusion of dissolved material through the grain boundary fluid, and (3) precipitation of the dissolved solid in grain boundaries under low normal stress or on free pore walls. A key question is whether a dynamically wetted island-channel network or fluid films can persist or will be eliminated by grain boundary healing phenomena (Hickman & Evans 1995). At very low differential stresses, surface energy effects are expected to play a significant role (Heidug 1995), causing such structures to neck-down to form isolated fluid inclusions with lower interfacial area, i.e. causing healing of the grain boundary (Houben et al. 2013) (see Figure 1d) and hence cessation of pressure solution creep at a threshold stress level (De Meer et al. 2002; Desbois et al. 2012; Van Noort et al. 2008).

Assuming a non-equilibrium, grain boundary island-channel structure, and examining competition between surface-energy-driven island growth (grain boundary healing) versus wetting of the grain boundary by undercutting (dissolution) of the islands, Van Noort et al. (2008) proposed a model defining a threshold grain boundary stress for pressure solution in porous quartz aggregates. This was expressed as an effective normal stress $\sigma_{crit} = \sigma_n - P_f$, where σ_n is the total normal stress component on a dissolving grain boundary and P_f is the fluid pressure in the connected island-channel structure. The quartz was assumed to be purely elastic, with dissolution of the load-supporting islands being driven by their average elastic strain energy. Below the "threshold stress" obtained, pressure solution is prevented as the fluid channel network becomes disconnected by surface-energy-driven grain boundary healing. The grain contact threshold stress for pressure solution in quartz, based on the model by Van Noort et al. (2008), is given by the criterion:

$$\sigma_{crit} = 2\alpha \sqrt{\frac{E\gamma_{sl}}{2r}\left(\cos\left(\frac{\theta}{2}\right) - \cos\left(\frac{\theta_{eq}}{2}\right)\right)} \tag{1}$$

Here α is the total island area fraction of grain boundary occupied by solid island contact, E the Young's modulus of quartz, γ_{sl} is the solid/liquid interfacial energy, r is the radius of interfacial curvature at island margins, θ is the dihedral angle at the contact margin (near 0° in dynamically wetted grain boundaries) and θ_{eq} is the dihedral angle at the contact margin at thermodynamic equilibrium. This criterion predicts grain contact threshold stresses for pressure solution in quartz that match favorably with those associated with cessation of pressure solution in hydrothermal compaction experiments on granular quartz aggregates reported by Niemeijer et al. (2002). Using the model of Van Noort et al. (2008), Desbois et al.

(2012) predicted that grain boundary healing in natural rock salt dominates over dynamic wetting when effective normal contact stresses on grain boundaries (assumed equal to differential stress) fall below 1-10 MPa, with the threshold value depending on the radius of curvature of grain boundary fluid inclusions or channels.
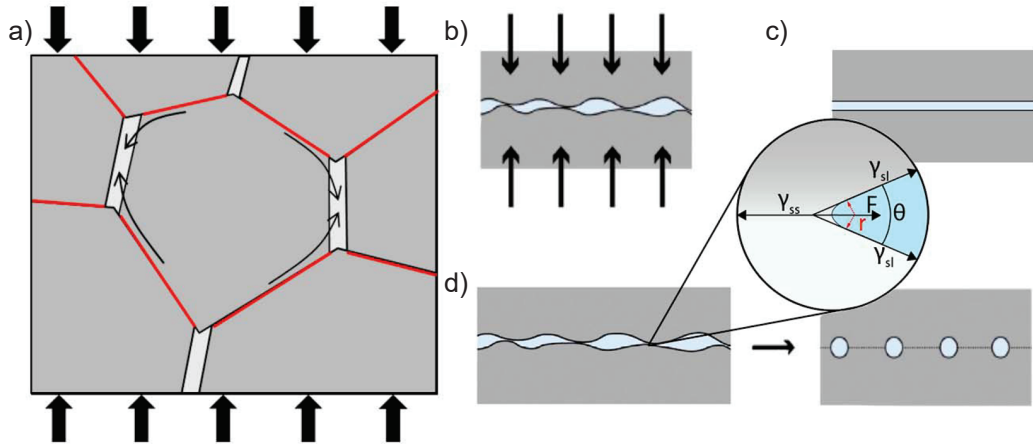

Figure 1: (a) Schematic diagram illustrating pattern of mass transfer involved in creep by pressure solution in a polycrystalline aggregate. Grain boundaries contain a fluid phase. Dissolution occurs at grain boundaries under high normal stress (red) followed by diffusion to and precipitation at grain boundaries under low normal stress (light grey). (b) An island-channel model of a fluid-filled grain boundary. (c) An adsorbed fluid film model of a grain boundary. (d) Necking down (occlusion) of a grain boundary channel network or fluid film to form arrays of disconnected spherical inclusions, by means of surface-energy-driven diffusive mass transport (Houben et al. 2013).

However, Desbois et al. (2012) do not take into account that: (1) stress intensification will occur at the tips of the generally elliptical fluid inclusions and channels found in salt grain boundaries (also ignored by Van Noort et al), (2) the radius of curvature appearing in the Van Noort criterion is the inclusion tip radius r (Figure 1d) as opposed to the much larger inclusion periphery or roof/floor radius, and (3) easy plastic deformation of salt compared with quartz means that the free energy (elastic strain energy) stored in dislocations produced by plastic deformation at island margins contributes to the chemical potential hence solubility of the solid islands, facilitating dissolution. When these three factors are considered, it is expected that a lower threshold stress will emerge for pressure solution in rock salt than predicted by Desbois et al (2012). In the following, we derive a revised expression for the threshold stress in salt, taking these factors into account.

3   Theoretical model

As starting point, consider a representative element of grain boundary (Figure 2) orientated normal to the maximum principal compressive stress (σ_1) in a volume of salt rock deforming by pressure solution but very close to the threshold stress at which grain boundaries heal. Grain boundaries are assumed to possess an island-channel structure that is still just connected. This means that the fluid pressure (P_f) within the channels will be buffered by and roughly equal to the minimum principal stress (σ_3), as grain boundaries generally have low tensile (hydrofracture) strength. The element considered in Figure 2 contains a single representative channel.

Given the above assumptions, the average differential stress experienced by the intervening solid islands (area fraction α) will be equal to $(\sigma_1 - \sigma_3)/\alpha$. With reference to Figure 2, the chemical potential of the solid at any point on a channel surface (or at any point on solid-solution interface) is given by the relation: $\mu_s \equiv \mu_{se} = f_s + P_f\Omega_s + \frac{\gamma_{sl}}{R_s}\Omega_s$ (Heidug 1995). Here μ_{se} is the equilibrium potential of the solute in the solution (by definition identical to the potential of the solid μ_s), f_s represents the Helmholtz free energy of the solid ($Jmol^{-1}$), P_f is the fluid pressure (Pa), Ω_s is the molar volume of the solid (m³ mol⁻¹), γ_{sl} is the interfacial free energy of the solid/liquid interface (Nm^{-1}) and R_s is the minimum principal radius of local interfacial curvature measured in the solid (m). For equilibrium at the triple junction contact between two grains (islands) and a fluid inclusion or channel, the Young-Dupré force balance: $\gamma_{ss} = 2\gamma_{sl}\cos\left(\frac{\theta_{eq}}{2}\right)$ applies, where γ_{ss} is the solid-solid interfacial free energy (Nm^{-1}) and θ_{eq} is the equilibrium dihedral angle. Based on the experiments of Lewis & Holness 1996, the equilibrium dihedral angle in rock salt is $60 - 70°$, for the halite-brine system at typical pressure-temperature conditions down to around $3\,km$ (though the uncertainties may be large, especially considering the effects of anisotropy in halite surface energy - Laporte & Provost 2000). When a fluid inclusion or channel is removed from equilibrium by undercutting of islands at triple junctions, the resulting dihedral angle $\theta \to 0$ and the thermodynamic surface force F (Nm^{-1}) acting on the triple junction or cusp sites A, (Figure 2) can be approximated by $F = 2\gamma_{sl} - \gamma_{ss}$.
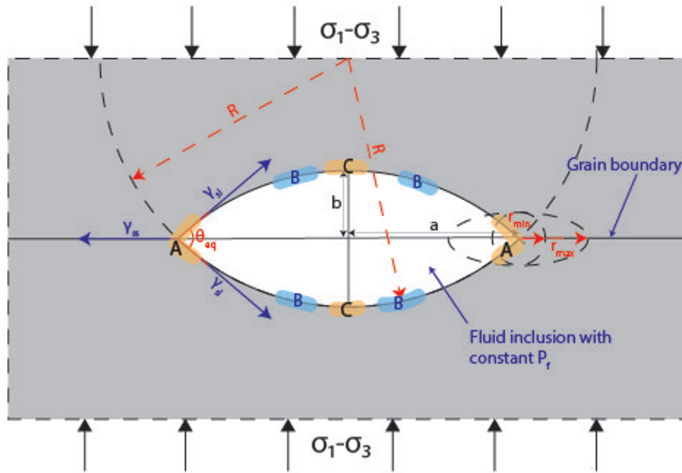

Figure 2: Schematic diagram of an elliptical inclusion or channel close to equilibrium in an element of grain boundary normal to σ_1 in a salt polycrystal where $\sigma_1 > \sigma_3 \approx P_f$. Aspect ratio a/b is defined by the equilibrium dihedral angle. At point A in the solid, there is intense concentration of vertical compressive stress, while at C there is horizontal extension. Point B is a neutral point where there is little or no deformation of the solid, relative to a hydrostatic reference state ($\sigma_1 = \sigma_3 = P_f$).

The above relations for the Young-Dupré Force F and for chemical potential are now applied to determine the chemical potential of the solid at sites A and B (Figure 2). From (2), the chemical potential of the solid at a neutral region B where there is no stress concentration (intermediate between the point of maximum compressive stress concentration at A and the maximum tensile stress at C) is given by $\mu_B = f_B + P_f\Omega_B - \frac{\gamma_{sl}\Omega_B}{R}$, where R is the radius of curvature of the fluid-solid interface measured in the fluid (Figure 2). At region A, the chemical potential is given by: $\mu_A = f_A + P_f\Omega_A - \frac{F\Omega_A}{2r}$ (Van Noort et al. 2008), in which r is the of curvature

within the dissolving cusp region during initiation of island undercutting (see Figure 2). This is taken to be at least equal to the radius of curvature at the tip of an ellipse (r_{min}) and at most to half the inclusion/channel height ($r_{max} = b$), so that: $\frac{b^2}{a} \leq r \leq b$. Assuming, the difference in molar volume between A and B is negligible, the potential difference between A and B is therefore given by:

$$\Delta\mu_{AB} = \mu_A - \mu_B = \Delta f_{AB} - \left(\frac{F}{2r} + \frac{\gamma_{sl}}{R}\right)\Omega_s \tag{2}$$

For dissolution at A (island undercutting and dynamic wetting), $\Delta\mu_{AB} > 0$. Recognizing that $R \gg r$, for typical dihedral angles, and that R/r will increase further as island dissolution proceeds, the criterion for non-equilibrium (dynamic) wetting versus healing of grain boundaries becomes:

$$\Delta f_{AB} > \frac{-F}{2r}\Omega_s = \frac{\gamma_{sl}\left[1-cos\left(\frac{\theta_{eq}}{2}\right)\right]}{r}\Omega_s \tag{3}$$

To obtain Δf_{AB}, the difference in local stress state between the cusp regions A and the neutral regions B is needed. Assuming that the stress concentration at cusp sites (A) leads to localized work hardening plastic flow, the stress at A can be crudely estimated using the stress intensification factor $\lambda = \left(1 + 2\frac{a}{b}\right)/\alpha$ at the tip of a 2D elliptical hole in an infinite elastic medium due to Inglis (1913), augmented by the additional factor $1/\alpha$ reflecting the effect of island area fraction. Our approximation for the stress at A is hence given by $\lambda\sigma/\alpha$, or $z\sigma$ where σ is the far field differential stress ($\sigma_1 - \sigma_3$) and $z = \lambda/\alpha$. For an equilibrium dihedral angle (θ_{eq}) of 60° (Lewis & Holness 1996), the geometry of Figure 2 under near-equilibrium conditions (near-uniform R) implies a (minimum) aspect ratio $\frac{a}{b}$ of 3.73, so that the stress intensification z at A is (8.46)/α or ~17 for $\alpha = $ ½, for example. During isothermal deformation of a solid, elastic and dislocation stored energy contribute to the local Helmholtz free energy (e.g. Lehner 1990; Peach et al. 2001, Van Noort et al. 2008), so that:

$$\Delta f_{AB} = \Delta f_{elastic} + \Delta f_{dislocations} \approx \left(\frac{(z\sigma)^2}{E} + \rho W\right)\Omega_s \tag{4}$$

where E is the Young's Modulus in Pa, ρ is the dislocation density in m^{-2} and W is the dislocation self-energy in Jm^{-1}. In addition, via: $\rho W = \beta\frac{(z\sigma)^2}{G}$, in which β is constant with a value of approximately one and G is the shear modulus (Hull et al. 2011), so that:

$$\Delta f_{AB} = (z\sigma)^2 \left(\frac{1}{E} + \frac{1}{G}\right)\Omega_s \tag{5}$$

Combining this with Eq. (3), the threshold differential stress for non-equilibrium grain boundary wetting, hence pressure solution in rock salt, can now be expressed as:

$$\sigma_{ps} = \sqrt{\frac{EG}{E+G}\frac{\gamma_{sl}}{r}\frac{1-cos\left(\frac{\theta_{eq}}{2}\right)}{z^2}} \tag{6}$$

This criterion represents an unstable equilibrium state from which the system will always evolve such that grain boundary wetting occurs when $\sigma_1 - \sigma_3 > \sigma_{ps}$ and grain boundary healing occurs when $\sigma_1 - \sigma_3 < \sigma_{ps}$.

4 Model predictions

Suitable parameter values are now inserted into Eq. (6) to predict the threshold stress σ_{ps} for pressure solution in salt rock at depths up to 3 km (lithostatic pressure 65 -70 MPa, 75-110 °C). Bruno et al. (2009) show that the salt-brine interfacial energy at 30 °C is 0.125 Nm^{-1} for (100), 0.270 Nm^{-1} for (110) and ~0.4 Nm^{-1} for (111). In this study, the most favorable value for wetting of 0.125 Nm^{-1} is used. Further, we take $E = 29\ GPa$, $G = 11\ GPa$ (Warren 2016), $\theta_{eq} = 60 - 70°$, and $r = 1 - 100\ \mu m$. The chosen value of z is based on the above analysis of stress intensification at island margin sites (triple junction or cusp region A, Figure 2) and taken as 10-20. The predicted dependence of σ_{ps} on cusp radius r is shown in Figure 3, along with a comparison with the threshold stress estimates by Desbois et al (2012).
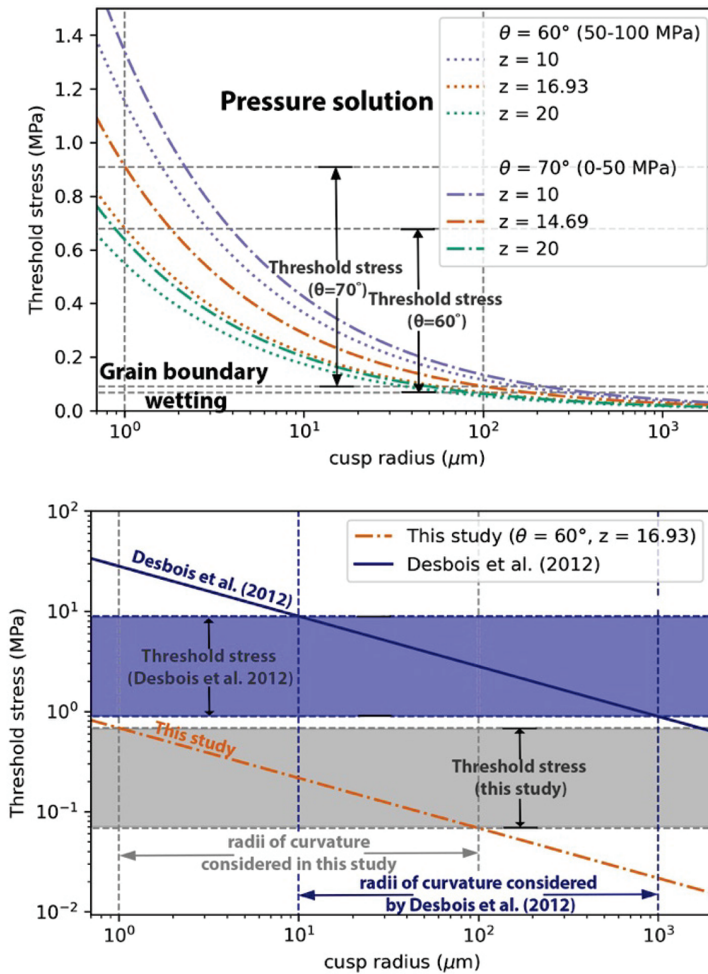

Figure 3: (top Predicted threshold stress for pressure solution vs.(log) cusp radius r for values of z between 10 and 20 and for $\theta_{eq} = 60°$ and 70°. (bottom) Equivalent log-log plot for parameter values expected at $\theta_{eq} = 60°$ and z = 16.93°,plus comparison with the threshold given by Desbois et al. (2012). N.B. The threshold stress is a threshold in differential or deviatoric stress.

Under ambient laboratory conditions, connected grain boundary fluid inclusions, films and channels in the Gorleben and Asse rock salt typically have a measured width (2b in Figure 2)

of 10 to $40\ \mu m$ normal to the grain boundary plane, while some isolated inclusions have diameters of up to $200\ \mu m$ in the Asse rocksalt (Urai et al. 1987; Thiemeyer et al. 2015), These values may be reduced under confined (e.g. in-situ) conditions, though this effect is expected to be minor (no change in order), especially when inclusions are brine filled. For inclusion widths in this full range of 10 to $200\ \mu m$, and corresponding aspect ratios ($\frac{a}{b}$, Figure 2) of 3.17 and 3.73, the relation $\frac{b^2}{a} \leq r \leq b$ given above yields radii of curvature (r) at the cusp between 1 and $100\ \mu m$. For this range in cusp radii, the threshold differential stress for pressure solution predicted by the present theory (Figure 3) is respectively $0.09 - 0.9\ MPa$ at shallow depths ($\theta_{eq} = 70°$, $P_c = 0 - 50\ MPa$) and $0.07 - 0.7\ MPa$ at deeper levels ($\theta_{eq} = 60°$, $P_c = 50 - 100\ MPa$) and assuming elliptical inclusion cross-section and an associated stress intensification z of 10 to 20. This is the stress required to activate grain boundary brine films and hence pressure solution in rocksalt. Note that it is at least one order lower than the estimate of $1 - 10\ MPa$ put forward by Desbois et al (2012) on the basis of the original (elastic) model by Van Noort et al. (2008) coupled with r-values corresponding to inclusion periphery or roof/floor radii (see Figure 3).

5   Comparison with microstructural constraints

The above estimates for the threshold differential stress for pressure solution are now compared with microstructural constraints on the stresses and deformation mechanisms operating during natural salt flow. The in-situ stresses driving flow of rock salt in nature cannot be measured directly. However, they can be estimated using the relationship between steady state flow stress $\sigma = (\sigma_1 - \sigma_3)$ and subgrain diameter d that all crystalline materials exhibit when deformation involves a component of dislocation creep (Twiss 1977). This relationship takes the form $d = K\sigma^{-m}$ where K and m are temperature-insensitive, material parameters (Twiss 1977). It was calibrated for natural and synthetic rocksalt in deformation experiments in the dislocation creep regime by Carter et al. (1993) yielding $K = 215$ and $m = 1.15$ (Urai & Schléder, 2005).

Now, subgrain sizes in naturally deformed rocksalt, from strongly deformed domal to lightly deformed bedded salt, typically vary from 80 to $360\ \mu m$ (e.g. Carter et al. 1982). Values around $200\ \mu m$ (stress ~1 MPa) are common in salt domes and walls, e.g. at Avery Island (Carter et al. 1982) and at Asse, Germany (Urai et al. 1987). Measured subgrain sizes in bedded rocksalt samples from Hengelo (Netherlands) show values in the range $290\ \mu m \pm 143\ \mu m$ to $390\ \mu m \pm 223\ \mu m$ (Schléder & Urai 2005). These data suggest that dislocation creep is active in all of the naturally deformed systems studied to date, although the strain contribution is unconstrained and may be small (a few% strain is sufficient to produce subgrains – e.g. Pennock et al. 2006). Using the above relationship between flow stress and subgrain size, the implication is that differential stresses in natural rocksalt lie between $0.4\ and\ 2.5\ MPa$. At the same time, many naturally deformed salts show evidence not only of dislocation creep (in the form of subgrains) but also of a) dynamic recrystallization involving fluid assisted grain boundary migration by dissolution-precipitation transfer across grain boundary brine films, and b) intergranular precipitation/overgrowth features suggesting pressure solution (Urai et al., 1987; Spiers & Carter, 1998; Schléder & Urai 2005). In addition, combined experimental plus microstructural studies performed on synthetic salt rock (Ter Heege et al. 2005; Pennock et al. 2006) have demonstrated that fluid-assisted dynamic recrystallization tends to occur in or near the transition between dislocation glide/creep and pressure solution. Taken together, the above pieces of evidence indicate that dislocation creep, fluid-assisted recrystallization and pressure solution occur alongside each other during natural salt flow at differential stresses in the range 0.4 to 2.5 MPa. This in turn implies that any threshold stress for pressure solution must lie at lower values, lending support to our model predictions of 0.07 to 0.70 (> 2km) or 0.90 MPa (<2 km) and providing a basis to reject the threshold of 1 to $10\ MPa$ estimated by Desbois et al (2012) as too high.

6   Implications for creep of natural rock salt

To assess the impact of the presently derived threshold for pressure solution on the creep behavior of rock salt at low deviatoric stresses in the further field around salt caverns, storage facilities and boreholes (and in the context of salt tectonic flow), we have added it to a deformation mechanism map for salt constructed using well-known dislocation creep (Hunsche and Hampel, 1999) and pressure solution (Spiers et al., 1990) creep equations (Figure 4). Inspection of Figure 4 shows that at 60-100°C, most natural salts, which have a grain size around $5 - 10\ mm$, are expected to show a transition from dislocation creep to pressure solution at stresses in the range $2 - 8\ MPa$ and strain rates in the range $10^{-11} - 10^{-13}\ s^{-1}$. These stresses fall above but close to those inferred from subgrain sizes measured for dynamically recrystallized salts with active fluid films, such as the Asse material (Urai et al. 1987) but a factor of $10 - 100$ times higher than the threshold stress for pressure solution predicted in this study. On this basis, combined with the microstructural arguments detailed above, we infer that at 2-3 km depth pressure solution can be expected to be active during flow of rock salt at stresses down to threshold values in our predicted range of $0.07 - 0.70\ MPa$. We anticipate that pressure solution strain rates may start to deviate from the Spiers et al. pressure solution law at $\sim 0.7\ MPa$, dropping to zero below $\sim 0.07\ MPa$, while dilslocation creep remains active but at rates   below $10^{-16} - 10^{-18}\ s^{-1}$, i.e. some 4-6 orders lower than if pressure solution were active (see Figure 4) This effect can be simplified by assuming a mid-range threshold of say $0.2\ MPa$ (horizontal black line in Figure 4b), above which pressure solution creep is unaffected and below which it is inhibited by grain boundary healing, causing an abrupt switch back to dislocation creep at strain rates some four to six orders of magnitude lower than expected for pressure solution at $0.2\ MPa$.
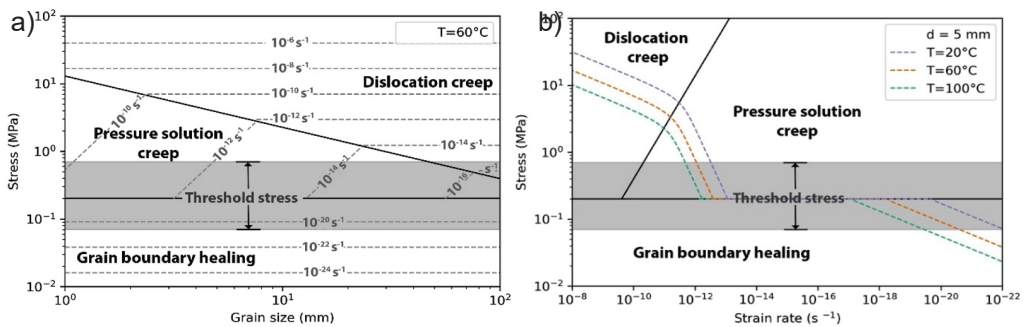

Figure 4: (a) Deformation map for rock salt drawn at a constant temperature of 60 °C in log grain size vs. log stress space. (b) Deformation map at constant grain size (d = 5mm) drawn in log strain rate vs. log stress space. Stresses are differential or deviatoric flow stresses. Creep rates are based on the dislocation creep law by Hunsche & Hampel (1999), and the pressure solution creep equation of Spiers et al. (1990). Below the threshold stress, pressure solution creep is inhibited, healing dominates and strain rates drop by 4-6 orders.

The impact that the threshold behavior captured in Figure 4 will have in numerical models addressing i) salt flow in the far field around solution-mined caverns, storage facilities and boreholes, and ii) the associated long-term system evolution and surface effects, remains to be seen. Qualitatively, though, the threshold can be expected to limit the radial extent of the zone around an opening in which pressure solution is active (depending on cavern pressure). The present threshold stress model is purely theoretical and needs to be tested in future by means of long-term experiments and direct micro-CT or optical observations of grain boundary behavior under increasing normal stress. If proven to exist, long-term, far-field modelling

clearly needs to consider not only pressure solution creep but also the measured value or range of the threshold stress observed.

7   Conclusions

This study has derived a theoretical criterion estimating the differential stress at which surface-energy-driven healing effects dominate over stress-driven dynamic wetting phenomena in brine-bearing grain boundaries in rock salt. Below this threshold stress, grain boundary brine channels disconnect, and pressure solution creep is inhibited. Our main conclusions are as follows:

- When the free energy of dislocations and stress intensification effects around grain boundary fluid inclusions and channels are considered, surface energy effects are expected to prevent pressure solution in salt below a threshold differential stress of 0.07 to at most 0.90 MPa (as opposed to earlier estimates of 1-10 MPa).
- Many naturally deformed rock salts display microstructural evidence for both dislocation creep and dissolution-precipitation mechanisms. Associated subgrain sizes, coupled with experimentally calibrated subgrain size vs. stress relations, imply flow stresses that are higher than the threshold stress derived here. This confirms that pressure solution creep can operate in natural rock salt above the calculated threshold.
- A decrease in strain rates from $\sim 10^{-13}$ to 10^{-18} s^{-1} is expected when deviatoric stresses in rock salt drop below the threshold value. At this point pressure solution creep ceases leaving only dislocation creep to operate at vanishingly low rates.
- The present threshold stress needs to be verified via suitable experiments.
- If verified, the effects of the present threshold stress for pressure solution need to be considered in future numerical studies of flow around salt caverns and storage facilities.

Acknowledgements

References

BÉREST, P., GHARBI, H., BROUARD, B., BRÜCKNER, D. DE VRIES, K., HÉVIN, G., SPIERS, C.J. & URAI, J. 2019. VERY slow creep tests on salt samples. Rock Mechanics and Rock Engineering, 52(9), 2917-2934.

BREUNESE, J.N., DE MEER, S. & KROON, I.C. 2003. Observation and prediction of the relation between salt creep and land subsidence in solution mining. The Barradeel case. In: Proc. SMRI Fall Meeting, Chester: United Kingdom. p. 38-57.

BRUNO, M. AQUILANO, D. & PRENCIPE, M. 2009. Quantum-mechanical and thermodynamical study on the (110) and reconstructed (111) faces of NaCl crystals. Crystal Growth and Design, 9(4), 1912-1916.

CARTER, N.L, & HANSEN, F.D. 1983. Creep of rocksalt. Tectonophysics, 92(4), 275-333.

CARTER, N.L., HORSEMAN, S.T., RUSSELL, J.E. & HANDIN, J. 1993. Rheology of rocksalt. J. Struct. Geol. 15 (9–10), pp. 1257–1271.

DE MEER, S., SPIERS, C.J., PEACH, C.J. & WATANABE, T. 2002. Diffusive properties of fluid-filled grain boundaries measured electrically during active pressure solution. Earth Planet. Sci. Lett. 200 (1–2), pp. 147–157.

DESBOIS, G., URAI, J.L. & DE BRESSER, J.H. 2012. Fluid distribution in grain boundaries of natural fine-grained rock salt deformed at low differential stress (Qom Kuh salt fountain, central Iran) : Implications for rheology and transport properties. Journal of Structural Geology, 43, 128-143.

HEIDUG, W.K. 1995. Intergranular solid-fluid phase transformations under stress: The effect of surface forces. J. Geophys. Res. Solid Earth 100 (B4), pp. 5931–5940.

HICKMAN, S.H. & EVANS, B. 1991. Experimental pressure solution in halite: The effect of grain/interphase boundary structure. J. Geol. Soc. London. 148 (3), pp. 549–560.

HERCHEN, K., POPP, T., DÜSTERLOH, U., LUX, K., SALZER, ET AL. 2018. WEIMOS : Laboratory Investigations of Damage Reduction and Creep at Small Deviatoric Stresses in Rock Salt. pp. 175-192.

HOUBEN, M.E., TEN HOVE, A., PEACH, C.J. & SPIERS, C.J. 2013. Crack healing in rocksalt via diffusion in adsorbed aqueous films: Microphysical modelling versus experiments. Phys. Chem. Earth 64, pp. 95–104.

HULL, D. & BACON, D.J. 2011. Introduction to dislocations (Vol. 37). Elsevier.

HUNSCHE, U. & HAMPEL, A. 1991. Rock salt—the mechanical properties of the host rock material for a radioactive waste repository. Eng. Geol. 52 (3), pp. 271–291.

INGLIS, C.E. 1913. Stresses in a plate due to the presence of cracks and sharp corners. Trans Inst Naval Archit, 55, 219-241.

LAPORTE, D. & PROVOST, A. Equilibrium geometry of a fluid phase in a polycrystalline aggregate with anisotropic surface energies: dry grain boundaries. Journal of Geophyiscal Research: Solid Earth 2000, 105. B11: 25937-25953.

LEHNER, F.K. 1990. Thermodynamics of rock deformation by pressure solution. In: McClay, K.R. (Ed.), Deformation Processes in Minerals, Ceramics and Rocks. pp. 296–331.

LEWIS, S. & HOLNESS, M. 1996. Equilibrium halite-H_2O dihedral angles: High rock-salt permeability in the shallow crust?. Geology 24 (5), pp. 431–434.

NIEMEIJER, A.R., SPIERS, C.J. & BOS, B. 2002. Compaction creep of quartz sand at 400–600 C: Experimental evidence for dissolution-controlled pressure solution. Earth and Planetary Science Letters, 195(3-4), 261-275.

ORLIC, B. & BUIJZE, L. 2014. Numerical modeling of wellbore closure by the creep of rock salt caprocks. In: 48th US Rock Mechanics / Geomechanics Symposium 2014. pp. 1533–1540.

PEACH, C.J., SPIERS, C.J. & TRIMBY, P.W. 2001. Effect of confining pressure on dilatation, recrystallization, and flow of rock salt at 150°C. J. Geophys. Res. 106 (B7), pp. 13,315-13,328.

PENNOCK, G.M., DRURY, M.R., PEACH, C.J. & SPIERS, C.J. The influence of water on deformation microstructures and textures in synthetic NaCl measured using EBSD. Journal of structural geology, 2006, 28.4: 588-601.

RAITH, A.F., STROZYK, F., VISSER, J. & URAI, J.L. 2016. Evolution of rheologically heterogeneous salt structures: a case study from the NE Netherlands. Solid Earth, 2016, 7.1, pp. 67-82.

RUTTER, E.H. 1976. The Kinetics of Rock Deformation by Pressure Solution. Philos. Trans. R. Soc. A Math. Phys. Eng. Sci. 283 (1312), pp. 203–219.

SCHLEDER, Z. & URAI, J.L. 2005. Microstructural evolution of deformation-modified primary halite from the Middle Triassic Röt Formation at Hengelo, The Netherlands. Int. J. Earth Sci. 94 (5–6), pp. 941–955.

SCHLÉDER, Z. BURLIGA, S. & URAI, J.L. 2007. Dynamic and static recrystallization-related

microstructures in halite samples from the Kłodawa salt wall (central Poland) as revealed by gamma-irradiation. Neues Jahrb. für Mineral. - Abhandlungen 184 (August), pp. 17–28.

Sᴘɪᴇʀs, C.J. & Cᴀʀᴛᴇʀ, N.L. 1998. Microphysics of rocksalt flow in nature. Aubertin, M., and Hardy, H.R. (eds.): The mechanical behavior of salt, proceedings of the 4th conference, Trans Tech. Publ. Series on Rock and Soil Mechanics, 22, 115-128.

Sᴘɪᴇʀs, C.J., Sᴄʜᴜᴛᴊᴇɴs, P.M.T.M., Bʀᴢᴇsᴏᴡsᴋʏ ,R.H., Pᴇᴀᴄʜ, C.J., Lɪᴇᴛᴢᴇɴʙᴇʀɢ, J.L. & Zᴡᴀʀᴛ, H.J. 1990. Experimental determination of constitutive parameters governing creep of rocksalt by pressure solution. Geological Society, London, Special Publications, 54(1), 215-227.

Tᴇʀ Hᴇᴇɢᴇ, J.H., Dᴇ Bʀᴇssᴇʀ, J.H.P. & Sᴘɪᴇʀs, C.J. 2005. Dynamic recrystallization of wet synthetic polycrystalline halite: Dependence of grain size distribution on flow stress, temperature and strain. Tectonophysics 396 (1–2), pp. 35–57.

Tʜɪᴇᴍᴇʏᴇʀ, N. Hᴀʙᴇʀsᴇᴛᴢᴇʀ, J., Pᴇɪɴʟ, M. Zᴜʟᴀᴜғ, G. & Hᴀᴍᴍᴇʀ, J. 2015. The application of high resolution x-ray computed tomography on naturally deformed rock salt: Multi-scale investigations of the structural inventory. Journal of Structural Geology, 77, 92-106.

Tsᴀɴɢ, C.F., Bᴇʀɴɪᴇʀ, F. & Dᴀᴠɪᴇs, C. 2005. Geohydromechanical processes in the Excavation Damaged Zone in crystalline rock, rock salt, and indurated and plastic clays in the context of radioactive waste disposal. International Journal of Rock Mechanics and Mining Sciences, 42(1), 109-125.

Tᴡɪss, R.J. 1977. Theory and applicability of a recrystallized grain size paleopiezometer. Pure Appl. Geophys. PAGEOPH 115 (1–2), pp. 227–244.

Uʀᴀɪ, J.L., Sᴘɪᴇʀs, C.J. & Zᴡᴀʀᴛ, H.J. & Lɪsᴛᴇʀ, G.S. 1986. Weakening of rock salt by water during long-term creep. Nature 324 (6097), pp. 554–557.

Uʀᴀɪ, J.L. Sᴘɪᴇʀs, C.J., Pᴇᴀᴄʜ, C.J. Fʀᴀɴssᴇɴ, R.C.M.W. & Lɪᴇᴢᴇɴʙᴇʀɢ, J.L. 1987. Deformation mechanisms operating in naturally deformed halite rocks as deduced from microstructural investigations. Geologie en Mijnbouw, 66(2), 165-176.

Vᴀɴ Nᴏᴏʀᴛ, R. Vɪssᴇʀ, H.J. & Sᴘɪᴇʀs, C.J. 2008. Influence of grain boundary structure on dissolution-controlled pressure solution and retarding effects of grain boundary healing. Journal of Geophysical Research: Solid Earth, 113 (B3).

Wᴀʀʀᴇɴ, J.K. 2016. Evaporites: A Geological Compendium, 2nd ed. Springer.